Axial Dispersion of Mass in Flow Through Fixed Beds

J. J. CARBERRY and R. H. BRETTON

Yale University, New Haven, Connecticut

The axial dispersion of water flowing through fixed beds was determined by measuring and recording the dispersion of a pulse input of dye at one or two points downstream of the injection site. Dispersion coefficients at various flow rates were obtained in systems of 1/2-, 1-, 3-, and 5-mm. spheres and 2- and 6-mm. rings each packed in a 1.5-in. I.D. column. Data were also obtained with 3-mm. spheres in a 1-in. I.D. column. Bed length was varied from 6 to 36 in. Void fractions of from 0.365 to 0.645 were represented by the systems studied. One gas system was studied at Reynolds numbers below unity.

The results of the water study indicate that the dispersion coefficient increases linearly with the Reynolds number in the range of Re = 0.5 to 100. Beyond that point the Reynolds number exponent decreases through 0.85 to a value of about 0.25 at a characteristic breakpoint in the region of Re = 350 to 400. Pressure-drop data secured for the systems studied clearly indicate that the cited breakpoint in dispersion behavior is identical with the well-known region of flow transition as characterized by the friction-factor–Reynolds-number relationship within a given system.

The dispersion values for the 5- and 6-mm. particles, while obeying this Reynolds-number functionality, are of lower magnitude.

A theory based upon bed-void cell-mixing efficiency is developed, and this efficiency is shown to be directly proportional to the Peclet number, which at the condition of perfect void-cell mixing should attain a value of about 2.

Anomalous behavior was noted in two respects: (1) the pulse amplitude change between two stations is greater than that predicted by either diffusion or cell-mixing theory, lending strong support to a bed-capacitance effect, and (2) short-bed studies revealed unusually high dispersion coefficients, reflecting short-circuiting, that is, poor cell-mixing efficiencies in these shallow beds, presumably owing to entrance effects, yet independent of the mode of pulse injection.

The dispersion of a pulse of air injected into a stream of helium flowing through a gas chromatographic column was briefly investigated. At $Re < 1$, E was found to be about equal to the calculated molecular diffusivity of this gas system.

In view of the key position occupied by fixed-bed processes in the chemical and allied industries, it follows that much attention should be focused on the fundamental aspects of heat, mass, and momentum transfer in these systems. Such studies are particularly important where heat and/or mass transfer occur simultaneously with one or more chemical processes. Ion exchange and catalyst regeneration constitute unsteady state examples, and any heterogeneously catalyzed reaction may be cited as a steady state case, in which the chemical kinetic picture is usually rendered more complicated by the transfer as well as the distribution of heat and mass.

With regard to mass transport there are aspects to be considered other than transfer or diffusion through a film to the surface of another contacting phase. There is the problem of fluid mixing across a packed bed (radial dispersion) and that of mixing in the axial or longitudinal direction of the bed.

Wilhelm and coworkers (*5*) initiated the experimental studies of radial dispersion of mass in packed columns, with the assumption, however, that the axial dispersion term in the basic differential equation could be neglected. This assumption was necessitated by a unique lack of data on axial dispersion, which is reflected in the fact that, to date, the design of fixed-bed reactors has been based upon the assumption that piston flow prevails in the system. The effect of axial dispersion in any reactor system is to damp the concentration gradient existing between bed inlet and outlet. As reaction or mass transfer rates generally depend upon the concentrations of reacting species at a point (for example, reactant concentration at the catalyst surface), it is apparent that axial dispersion reduces the conversion per pass simply because point concentrations are lower than those predicted on the assumption of piston flow. While designers are aware that packed beds exhibit axial mixing characteristics which lie between piston flow and those of perfect mixing, such as occurs in a well-stirred autoclave, the quantitative generalizations do not exist to permit the inclusion of the axial dispersion factor into rational design methods.

J. J. Carberry is with E. I. du Pont de Nemours and Company, Inc., Wilmington, Delaware.

EXPERIMENTAL APPROACH

An experimental study of axial dispersion implies immediately that the fluid employed be tagged at some point. The tagged portion of fluid is then the input signal to the system under study. Events which occur within the system (the packed column in this case) alter the input signal so that the character of the resulting output signal represents the response to the system.

The usual approach to the problem is essentially that of proposing a mathematical model *a priori* and then solving the basic equation for rational boundary conditions. The solution to this mathematical model for the signal imposed is then tested for agreement with the experimental results. If agreement is satisfactory, suitable constants or a particular coefficient are then obtained. Correspondence between the data and the theoretical equation does not necessarily prove that the model truly represents the physical system. Rather it may only demonstrate that the theoretical relation reproduces a result which is due to a reality more complicated than or even quite different from the assumed model. A classic example of this situation is the two-film theory of mass transfer. While it undoubtedly is a good working model in that field, radically different models are equally justified by mass transfer data at this time.

Of the three types of input signals (the step, pulse, and sine wave) which might be employed in a dispersion study, the pulse input was chosen in this work by virtue of the relative simplicity of equipment required. Further, both Kramers and Alberda (*13*) and Raseman and Bretton (*6*) have noted apparent discrepancies in the results acquired in the use of a sinusoidal signal.

In the present work the mathematical model chosen is one which has been used by other investigators. It is assumed that dispersion can be expressed by a simple diffusion type of equation. This model and one involving void-cell mixing are more fully discussed later in this paper. Strong evidence indicates that this diffusion model does not adequately describe the axial-dispersion phenomenon, however, the anomalous behavior observed may be due to necessary oversimplifications as well as to the choice of boundary conditions. Boundary conditions are quite critical, particularly in the case of short-bed studies. Further work is needed to define axial dispersion for short beds. Until such knowledge is secured, the data presented in this paper should be utilized with regard to the assumptions implicit in the model.

PREVIOUS STUDIES

Experimental studies of axial dispersion are of very recent origin, owing perhaps to the fact that rapidly responding measuring techniques are required in order to obtain an accurate account of the response of a system to an imposed signal.

Liquid Studies

Rafai (*15*) studied the dispersion of salt in water in laminar flow through sand beds ($Re < 1$), using a step input of salt solution and measuring the dispersion of the front directly in the bed at various bed lengths both chemically and by electric conduc-

tivity. The breakthrough data were treated by trial and error by the simple approximation which holds beyond several mixing lengths

$$C/C_0 = \tfrac{1}{2}[1 - \text{erf}\ (X - vt)/2(Et)^{\frac{1}{2}}] \qquad (1)$$

The two methods of measurement gave significantly different results, and arguments presented indicate that the electric-conductivity measurements made in the bed are not reliable.

Beran (*4*), who made a theoretical and limited experimental study of axial dispersion in a sand-packed column, showed that theoretically, for a pulse input, the dispersion coefficient could be obtained from the standard deviation of a measured Gaussian response, that is, if the dispersed pulse exhibits Gaussian character, its standard deviation σ is related to the Peclet number, column height L, and particle diameter D_p by the equation

$$\sigma = \sqrt{(2LD_p)(1/Pe)} \qquad (2)$$

Beran showed that this relationship applies when molecular diffusivity is insignificant. He reports the results of seven experimental runs in which a pulse of radioactively-tagged solution was injected into water flowing through a packed column (Re = 0.2 to 4.5). In the range of variables investigated he found the Peclet number to be a constant.

The first published result on axial dispersion in a packed bed appears to be that of Danckwerts (*8*). Although the paper is devoted largely to a theoretical discussion of residence-time distribution in flow systems, a single experiment is briefly described in which a step input of tracer was introduced into a bed packed with ⅜-in. Raschig rings. The fluid flowing was water at Re = 40. Danckwerts analyzed the breakthrough curve by means of the same equation employed by Rafai, that is, Equation (1).

Kramers and Alberda (*13*) followed Danckwerts's study with a theoretical and experimental investigation of axial dispersion as determined by the response of a packed column to a sinusoidal input signal. Theirs is the first discussion of the problem of axial dispersion in which an analogy is explicitly stated to exist between a packed bed and a series of mixing vessels. Relationships for the amplitude change and phase shift were obtained both for this model and also for the model based on a diffusion mechanism. It was shown that for a large number of mixers the two solutions gave the same frequency-response diagram. Experimentally, Kramers and Alberda investigated the dispersion in water flowing through a column packed with 1-cm. Raschig rings at Re = 100 and 200. In commenting upon the experimental results, they note that the phase-shift data indicate a lower value of n ($= Lv/2E$) than do the amplitude-change data. They describe the discrepancy as probably "being caused by a certain amount of trapping in the interior of the rings" (*13*). Their amplitude- and phase-shift data yield dispersion coefficients which differ by 50 to 100%.

Klinkenberg and coworkers (*12, 19*) have published two papers devoted to factors which affect residence-time distribution in vessels. Their discussion is confined to cases where the resulting distribution curves are Gaussian; that is, a large number of stages are involved. They attempt to treat cases where several events such as absorption, reaction, and mixing contribute to the net dispersion of a pulse. Klinkenberg (*12*) also cites the results of axial-dispersion measurements for flow in a sand bed made with the step-input technique ($Re < 1$).

Gas Studies

McHenry and Wilhelm (*14*) report axial-dispersion data for gas flowing through a bed packed with 3-mm. spheres. They used a sinusoidal-input signal and determined values of E from the amplitude change. A value of the Peclet number equal to about 2 was found in a Reynolds-number range of from 26 to 1,000, this value as has been shown (*2, 7*), being the limiting one corresponding to a mixing efficiency of 100% in each void cell of the bed.

In a recent theoretical discussion Aris and Amundson (*2*) demonstrate that the dispersion of a mathematical pulse by turbulent diffusion and dispersion by cell-mixing mechanisms are identical when complete cell mixing is assumed. A comparison of these distribution functions led them to conclude that the limiting value of the Peclet number at high Reynolds numbers should be about 2. One of the present authors (*7*) has shown that the Peclet number itself is a direct measure of void cell-mixing efficiency and that, while a value of Pe = 2 represents perfect void-cell mixing, values of Pe much less than 2 can be anticipated in the usual range of packed-bed-flow rates.

The results of the cited experimental investigations are discussed and noted graphically later in this paper. It is sufficient to note here that whereas the work of McHenry and Wilhelm (*14*) on gas dispersion embraced a wide range of flow rates, the data secured by others for liquid systems are confined to limited regions of the Reynolds number. Therefore, it was the purpose of this research to ascertain the behavior of the dispersion coefficient for water over a wider range of flow rates in beds of various particle size, length, and diameter. In addition, it was deemed important to determine the dispersion characteristics of a gas system in the Reynolds-number range below that studied by McHenry and Wilhelm (*14*).

THEORY

Ergun (*9*) provided substantial evidence for the existence of near-perfect mixing in some fixed-bed studies.

The other extreme, that of piston flow in any packed bed (E = 0), is virtually nonexistent. This may be shown as follows. Any packed bed must consist of a series of randomly arrayed void cells. The behavior of a pulse input imposed upon such a series of cells, each of holding time θ_n, will be considered.

The concentration-time behavior in the effluent of the nth perfect mixing cell is given by

$$C = \frac{G}{\theta_n{}^n} \frac{t^{n-1}e^{-t/\theta}}{(n-1)!} \qquad (3)$$

where G is the transform of an impulse function.

For several beds of the same total retention time T, the cell-holding time is obviously $\theta_n = T/n$. Equation (3) has been solved for equal total-volume beds composed of 2, 4, and 12 perfect mixers. The resulting dispersions are plotted in Figure 1. It is apparent that the least dispersion occurs when n is largest. The limit is the case of n approaching infinity. Since any real bed consists of a finite number of cells, it is clear that even in the limiting case of perfect mixing in each void cell there exists, nevertheless, a finite axial dispersion; hence, for a bed of many perfect mixing cells the axial dispersion of matter corresponds to a finite value of E.

One may infer that E is inversely related to cell mixing efficiency, which is a function of turbulence and retention time for a given fluid. Since fluid velocity and cell size may control mixing efficiency, as an approximation it may be assumed that

$$E = kD_pv \qquad (4)$$

The ratio $D_pv/E = 1/k$ is defined as the Peclet number, Pe.

Imperfect mixing may be viewed profitably as the result of by-passing or short-circuiting and dead-space retention. This simply states that of a given number of particles entering a void cell, a fraction pass through the cell in a time much shorter than the holding time, while another fraction is retained for a period much greater than this holding time. Obviously a distribution of retention times results, which is characterized by a dispersion coefficient E.

Drawing an analogy between this mechanism of imperfect mixing and Einstein's kinetic diffusion model, one of the authors showed (*7*) that

$$n = \frac{Lv}{2E} \qquad (5)$$

and consequently the height of a mixing unit is

$$\text{HMU} = 2E/v \qquad (6)$$

In a bed in which each cell is a perfect mixer, the length of each perfect mixing cell, according to the work of Aris and Amundson (*2*), will be some fraction γ of particle diameter D_p. This fraction γ will be about unity or less, depending on the packing arrangement. Thus the number of perfect mixers is $n_p = L/(\gamma D_p)$. For any bed one may define a cell-mixing efficiency as the ratio of actual mixers n to the limiting number in the perfect-mixing-cell case n_p:

Mixing efficiency, $\epsilon = n/n_p$; thus

$$\epsilon = (Lv/2E)/(L/\gamma D_p) = \gamma D_pv/2E$$

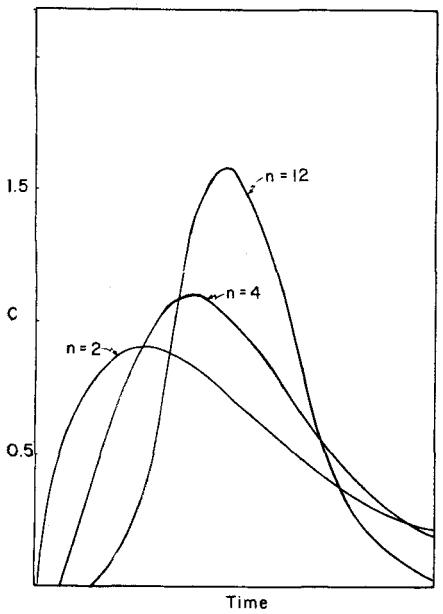

Fig. 1. Pulse dispersion in n perfect mixers. Equal total holding time.

or

$$\epsilon = (\gamma/2)Pe \qquad (7)$$

As γ is a constant for a given fixed bed the Peclet number is a direct measure of cell-mixing efficiency.

Further, the limiting value of the Peclet number is easily predicted from the foregoing argument, for as each void approaches the perfect-mixer ideal, $\epsilon \rightarrow 1$ and

$$Pe = 2/\gamma \qquad (8)$$

Since γ is approximately 1, the limiting value of the Peclet number is about 2.

Mathematical Model

This mixing-cell concept would imply that the spread of an injected tracer as a result of passage through a packed bed could be described by Equation (3). The application of this equation to experimental concentration-time data for a determination of n, and thus $E(= Lv/2n)$, would clearly be a most difficult task with beds of any reasonable length. For example Dankwerts (*8*) in a study of axial dispersion in a column packed with Raschig rings found n to be about 40.

An alternative approach is one employed by others who have studied the general problems of turbulent dispersion, that is, considering the problem in terms of Fick's Second Law of Diffusion:

$$E\frac{\partial^2 C}{\partial Z^2} = \frac{\partial C}{\partial t} \qquad (9)$$

where E, a dispersion coefficient, replaces the molecular diffusion coefficient.

Clearly, mass dispersion does not depend upon the concentration gradient as stated in Equation (9). Briefly, the justification for the use of Fick's Law is that its solution is identical with the solution of the more complex equations derived from statistical considerations of turbulence at points removed some distances from the injection site. Beeton (*3*) has treated this problem by developing from theoretical considerations a general expression governing the turbulent diffusion of mass from a point source. He shows that the distribution at points some distance downstream of the source can be reduced to a relatively simple equation, which is the solution of Fick's second-law expression. Beeton states, "In comparison with the accurate values obtained by graphical integration of this expression [the rigorous solution], the approximate equation is found to give better than 1 percent accuracy at all points beyond about 5 mixing lengths downstream of the source (*3*)."

As Aris and Amundson (*2*) have demonstrated the equivalence of the cell-mixing and turbulent-diffusion models at large values of n, then the use of a diffusion model for beds of many mixers satisfies the demands of both the statistical-turbulence and the cell-mixing theories.

Mathematical Treatment

In a differential segment of bed length, dX, through which a tracer of concentration, C, is being transported by a fluid flowing at a constant average velocity v and dispersed in the axial direction only at a rate governed by a mixing coefficient E, by material balance

$$E\frac{\partial^2 C}{\partial X^2} - v\frac{\partial C}{\partial X} = \frac{\partial C}{\partial t} \qquad (10)$$

If

$$Z = X - vt$$

and

$$t = t$$

then

$$E\frac{\partial^2 C}{\partial Z^2} = \frac{\partial C}{\partial t} \qquad (11)$$

Boundary Conditions

$$C(Z, 0) = 0 \begin{cases} 0 < Z < \infty \\ 0 > Z > -\infty \end{cases} \qquad (12)$$

and at $Z = 0$ there is an ∞ pulse of zero thickness.

$$\lim_{Z\rightarrow\infty} C(Z, t) = 0 \quad t > 0 \qquad (13)$$

and

$$Q = \pi r^2 f \int_{-\infty}^{\infty} C(Z, t)\, dZ \qquad (14)$$

where Q is the amount of tracer injected at $X = 0$ across a bed of cross-sectional area πr^2 and void fraction f. Equation (14) merely states that at any time for an infinite bed the total mass injected must be present in the bed. Boundary condition (13) implies that the bed is long or that the behavior at the end of a finite bed is the same as at a point L in an infinite bed. Equation (12) assumes a bed extended to $-\infty$. The final solution of Equation (11) with the boundary conditions given is

$$C(Z, t) = \frac{Q}{2\pi r^2 f\sqrt{\pi E t}} e^{-Z^2/4Et} \qquad (15)$$

Letting $K' = Q/(2\pi r^2 f)\sqrt{\pi}$ one obtains

$$C = \frac{K'}{\sqrt{Et}} e^{-Z^2/4Et} \qquad (16)$$

For a given E, the concentration-time profile is described by

$$C = \frac{K}{\sqrt{t}} e^{-Z^2/4Et} \qquad (17)$$

where

$$K = K'/\sqrt{E}$$

The time at which the maximum occurs is obtained by setting the first derivative dC/dt equal to zero. One obtains for t_m, the time at which C_{max} appears,

$$t_m = -E/v^2 + E/v^2(1 + (Xv/E)^2)^{\frac{1}{2}} \qquad (18)$$

when

$$(Xv/E)^2 \gg 1$$
$$t_m = X/v - E/v^2 \qquad (19)$$

As X/v is the nominal holding time, then as a result of dispersion the dispersed-pulse maximum actually arrives at the point of observation earlier than the residence time by an amount governed by E/v^2.

Discussion of Assumptions Implied in the Mathematical Model

It is clear that Equation (10) and its solution, Equation (15), involve the assumptions of (1) absence of radial gradients, (2) absence of bed capacitance, and (3) injection of a mathematical pulse, that is, a pulse of tracer of virtually zero thickness.

Radial Gradients

Smith and coworkers (*17*) have demonstrated that unusual radial-velocity profiles are encountered in the flow of gases through packed beds. They attributed these apparent anomalies to variation of void fraction with radial position in the beds studied. Thus it is to be expected that radial gradients of some magnitude will inevitably be present. However it is argued that if radial gradients are severe, one would then not expect the experimental concentration-time curves, at the observation points, to agree with the theoretical equation [Equation (15)], which is based upon the assumption of the

absence of such gradients. This is not to argue that a good fit of the data by the use of the theoretical equation is proof of the absence of radial gradients; rather it is to submit that a good agreement between data and theory simply means that whatever contribution radial gradients may make to axial dispersion is in fact well described by the dispersion coefficient E.

Bed Capacitance

Two stations of observation will be considered and Equation (15) applied to each and solved for E.

$$E = \frac{1}{4} \frac{(Z_1^2/t_1 - Z_2^2/t_2)}{\ln \sqrt{t_2/t_1} - \ln (C_1/C_2)} \quad (20)$$

Now when Z_1 and $Z_2 = 0$

$$C_1/C_2 = (t_2/t_1)^{\frac{1}{2}} \quad (21)$$

Thus the pulse amplitude should decrease as a function of the square root of time in the absence of capacitance effects, since the implication of Equation (20) is the equality $K_1 = K_2$. Two possible interpretations of an inequality of K_1 and K_2 are (1) variation of E with distance or (2) a decrease in Q due to column holdup or capacitance. The latter states that the signal entering bed 2 in a two-station system is not identical in total tracer mass Q to that which entered the preceding bed, since a finite capacitance in bed 1 withholds a fraction of the original signal. This does not necessarily imply a permanent adsorption on, or complete removal by, the packing but rather a trapping of fluid in low-velocity or stagnant areas from which removal occurs by a much slower mechanism than the primary dispersion one. This phenomenon should be evidenced by the existence of a long "tail" in the concentration-time profile.

Actually one can verify whether an abnormal amplitude ratio is due to variation in E or capacitance by use of two-station experimental data. Consideration of Equation (15) at $Z_1 = 0$ gives at the first station

$$C_1 = K_1/(t_1)^{\frac{1}{2}}$$

and at the second station

$$C_2 = K_2/(t_2)^{\frac{1}{2}}$$

from which values of K are directly obtained. If then the station 1 data are fitted for a particular value of E

$$C_1 = \frac{K_1}{(t_1)^{\frac{1}{2}}} e^{-Z_1^2/4E_1t_1} \quad (22)$$

and the same value of E fits the data of station 2 with

$$C_2 = \frac{K_2}{(t_2)^{\frac{1}{2}}} e^{-Z_2^2/4E_1t_2} \quad (23)$$

where

$$K_2 < K_1$$

Then it is clear that the inequality of K values must be a reflection of differing input signals due to capacitance. For if station 2 data were treated by use of a value of $E_2 > E_1$ in order to account for the inequality of K values, then

$$C_2 = \frac{K_1}{(t_2)^{\frac{1}{2}}} \left[\frac{E_1}{E_2}\right]^{\frac{1}{2}} e^{-Z_2^2/4E_2t_2} \quad (24)$$

would be the correlating relationship. Evidently Equations (23) and (24) yield different concentration-time distributions.

Pulse Injection

A consideration of the boundary conditions employed in the solution of the basic differential equation suggests the injection of a mathematical pulse input, that is, a pulse of zero thickness. Such an input signal cannot be physically realized; rather, any injected pulse will be of finite thickness. A solution to Equation (11) based upon a "thick" pulse input will, then, be considered. For a pulse of thickness $2a$ the boundary conditions are

$$C(Z, 0) = C_0 \quad -a < Z < +a$$

$$C(Z, 0) = 0 \quad \begin{cases} -\infty < Z < -a \\ +a < Z < +\infty \end{cases} \quad (25)$$

$$\lim_{Z \to \infty} C(Z, t) = 0 \quad t > 0 \quad (26)$$

$$Q = \pi r^2 f 2a C_0$$

$$= \pi r^2 f \int_{-\infty}^{\infty} C(Z, t)\, dZ \quad (27)$$

Equation (11) is satisfied by the expression

$$C = \frac{1}{2(\pi E t)^{\frac{1}{2}}} \cdot \int_{-\infty}^{\infty} F(Z') e^{-(Z-Z')^2/4Et}\, dZ' \quad (28)$$

since the integral does converge. The solution to these systems of equations is

$$C = -\frac{C_0}{2} \operatorname{erf}\left[\frac{(Z-a)}{2(Et)^{\frac{1}{2}}}\right] + \frac{C_0}{2} \operatorname{erf}\left[\frac{(Z+a)}{2(Et)^{\frac{1}{2}}}\right] \quad (29)$$

or

$$C = \frac{Q'}{4a}\left(\operatorname{erf}\left[\frac{Z+a}{2(Et)^{\frac{1}{2}}}\right] - \operatorname{erf}\left[\frac{Z-a}{2(Et)^{\frac{1}{2}}}\right]\right)$$

where

$$Q' = \frac{Q}{\pi r^2 f}$$

If Q' is allowed to remain constant as $a \to 0$, then by L'Hospital's Rule,

$$C = \frac{Q'}{2(\pi E t)^{\frac{1}{2}}} e^{-Z^2/4Et}$$

which is identical to Equation (15).

In a consideration of the behavior of Equation (29) in view of establishing the conditions under which it will reduce to Equation (15) for a given input pulse of thickness $2a$, Equation (29) at $Z = 0$ becomes

$$C = \frac{Q'}{2a} \operatorname{erf} \frac{a}{2(Et)^{\frac{1}{2}}} \quad (30)$$

If the error function is expanded in a series and only the first term of the series is used, Equation (30) becomes

$$C = Q'/[2(\pi E t)^{\frac{1}{2}}] \quad (31)$$

Equation (31) is the same expression obtained from Equation (15) at $Z = 0$. Thus for finite-width pulse injection one merely has to provide enough time (distance) between injection point and initial station of observation to render the second and succeeding terms in the series expansion of the error function insignificant and thus justify the use of the simpler Equation (15) in treatment of the experimental data.

EQUIPMENT AND MATERIALS

The test column consisted of sections of Dow-Corning glass pipe joined as required by a standard Corning bolt-and-flange assembly. The test section itself comprised an injector bolted between flanges and seated immediately atop the first packed test section of the bed, as well as the items described below. Between the end

TABLE 1. CHARACTERISTICS OF SYSTEMS STUDIED

Key: I.D. = nominal inside diameter of column, in.
f = percentage void volume of bed

System	I.D.	A	f	X_1	X_2
A-3 3-mm. spheres	1.5	11.4	37	61.3	91.8
B-5 5-mm. spheres	1.5	10.4	39	61.3	91.8
C-½ ½-mm. spheres	1.5	11.4	37	15.3	46
D-6 6-mm. rings	1.5	10.4	64.5	61.3	91.8
E-2 2-mm. rings	1.5	11.4	42.7	15.5	
F-1 1-mm. spheres	1.5	11.4	36.5	15.5	
G-3 3-mm. spheres	1.5	11.4	37.2	15.6	
H-3 3-mm. spheres	1.5	11.4	37.2	31.1	
I-3 3-mm. spheres	1	5.02	39	31.1	

(bottom) of the first bed and top of the second bed a ½-in.-high, clear-glass spacer was inserted, serving as the unpacked gap required for station 1 dye detection. An identical spacer was bolted between the bottom of the second bed and the downstream sections of unpacked pipe. The second spacer served as an optical window for station 2. Piping above the injector and test section provided the head requirement.

A constant-head weir was provided atop the entire column assembly. Water was supplied from the sink tap and conveyed by plastic garden hose up to the inner bowl of the weir assembly. Overflow was returned through four drain hoses to the laboratory sink. Downstream of the test section a horizontal run of pipe led to the sink. Volumetric flow rates were measured and regulated at this point.

An auxiliary line served as a means to fill and backwash the column. Backwashing was required to remove any trapped air from the packing. Packing in the test section was secured between support screens. Thus the beds were fixed and could not expand even under backwashing. This was done to ensure constancy of void fraction as originally determined upon initial packing of the sections.

Figure 2 is a schematic diagram of the experimental equipment. The pulse injector was designed to facilitate pulse injection either when the fluid was at rest (static injection) or when flow prevailed (dynamic injection). While static injection was employed in most of the runs, several dynamic injection runs were made to demonstrate that the results are independent of the mode of injection. In essence the technique consisted of rotating of *wafer* of dye solution into a small chamber between two packed sections.

Two 150-watt projector lamps were employed as light sources. Power was supplied to the lamps from a Variac in series with a voltage stabilizer. The lamp-lens system was modified empirically to obtain parallel light beams. Each lamp was placed upon a shelf mounted upon a wood frame surrounding the column. The heights of the two shelves were adjustable to accommodate various station positions. The light beam from each lamp focused directly upon the spacer at the respective stations. The lamp side of each spacer was masked so that a beam of light about 3-mm. thick and 25-mm. wide was transmitted through the gap at each station. Directly behind the column, in line with the light beam and on the same shelf with the lamp, the photocell box was located. A 929 RCA photocell was mounted in each of the two boxes. A window in each box (3 mm. high and 13 mm. wide) permitted passage of the light from the column gap to the photocell.

Photocell output was amplified by use of a simple cathode follower circuit, the output being impressed upon a dual channel Brush oscillograph.

Tap water was the liquid investigated with du Pont Pontamine Blue dye employed as tracer material. The molecular diffusivity of this dye is reported to be 5×10^{-6} sq. cm./sec. (*10*).

In the gas runs helium as a carrier gas was tapped directly from a high-pressure cylinder, and air, injected by a hypodermic needle, served as the tracer substance.

A gas chromatographic column several meters in length was employed for the gas studies, and a standard thermal conductivity cell detected the air pulse.

The essential characteristics of the systems studied are summarized in Table 1.

TREATMENT OF DATA

Early in the investigation analysis of two-station data clearly revealed that the maximum in the concentration-vs.-time plot

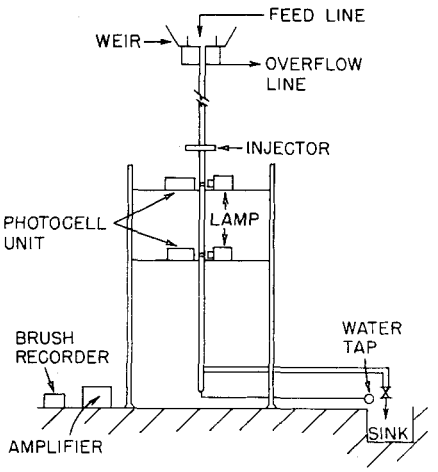

Fig. 2. Equipment layout.

did not decrease with an increase in bed length as predicted; in fact the amplitude decrease was greater than predicted. This fact, coupled with clear evidence of long "tails" in the concentration-time profile, suggested a capacitance effect which could not be accounted for by any single mechanism over the range of variables studied. Individual treatment of data at each of two stations did indicate that Equation (17) could be fitted to the data with success and that the same value of E fitted both station data provided the constant K was determined at each station.

With a previously determined calibration curve the Brush pen position at various chart positions was translated into dye concentration and chart position was converted to time coordinates by the known chart speed. The resulting concentration-time curve at a given station then had to be treated further with respect to the time axis. Two time corrections are involved, (1) a correction for residence time outside the bed and (2) a correction resulting from the shift in the maximum of the pulse due to the dispersion; that is, the maximum occurs not at the time $t = X/v$ but at $t_m = X/v - E/v$. An estimate of E is required, therefore, before one may treat the concentration-time curve for a final determination of E. Such an estimate can be obtained by use of an approximation valid for a Gaussian distribution (*18*). With the expression for C as a function of t for a given X and v [Equation (17)], one calculates a C-vs.-t curve for a specific value of E and the corrected t values. The coefficient K is readily determined from the original data, since at $X = vt'$ or $Z = 0$

$$K = C\sqrt{t'}$$

If a poor fit is obtained with the initially chosen value of E, another choice is made, the time values are recorrected in conformity with the corrections demanded by the term E/v^2, and another series of C-vs.-t values is calculated.

RESULTS

The method of presentation of data and results is:

1. The nine systems studied are designated by the letters A to I inclusive. Thus system A-3 refers to the experiments with the 3-mm. spheres in the 1.5-in. I.D. column. Table 1 summarizes the characteristics of each system.
2. Typical experimental results are

TABLE 2. TYPICAL EXPERIMENTAL DATA AND RESULTS

System	Run	v	E	Re	Pe
A-3	13	3.32	2.3	100	0.435
	32	11.3	5.8	340	0.59
	39	0.71	0.5	21	0.42
	51	16.4	6.5	490	0.76
B-5	63	20.7	8	1035	1.3
	66	15	7.2	750	1.04
	68	10.3	6.1	515	0.85
	70	5.1	4	254	0.64
	74	0.88	0.8	44	0.55
C-½	96	1.4	0.21	7.1	0.34
	102	3	0.45	15	0.33
	115	0.09	0.009	0.44	0.49
D-6	124	3.13	2.3	187	0.81
	128	0.57	0.44	34	0.78
	139	7.25	4.25	435	1
	143	19.7	10	1180	1.2
E-2	145	7	5.75	140	0.2
	147	1.4	1	28	0.28
	152	18.5	10	370	0.37
	155	0.45	0.2	8.9	0.44
F-1	164	0.14	0.038	1.4	0.37
	167	4.7	2	47	0.235
	171	10	4.5	103	0.23
G-3	182	0.67	0.5	20	0.4
	183	23	13	690	0.53
H-3	190	9	7.5	270	0.36
	191	2.84	2.8	85	0.3
	193	0.38	0.24	11	0.46
I-3	219	22.2	13	665	0.51
	221	7.9	7.25	240	0.33
He-air		0.3	0.4	0.046	0.015
		2.7	0.5	0.42	0.1

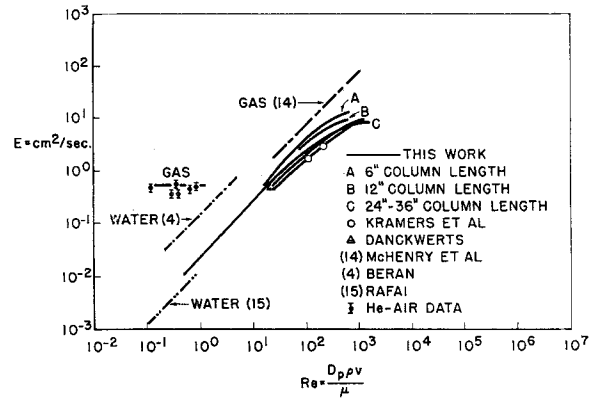

Fig. 3. Axial dispersion coefficient E, vs. Reynolds number.

given in Table 2.* Included are the run numbers in each system and particle diameter specified by the number following the system letter. For each run Table 2 lists bed velocity v, axial dispersion coefficient E, and Peclet and Reynolds numbers.

3. A complete graphical description of the results of this study as well as those of previous investigators is given in Figure 3 as a log-log plot of E vs. Re. A similar but more limited plot showing a portion of the data points for this work is given in Figure 4.

4. In Figure 5 the relationship between Pe and Re, for this and previous investigations is shown on logarithmic coordinates.

5. In Figures 6 and 7 both the experimental and theoretical concentration-time profiles for a few typical runs are reproduced.

6. Friction factor data are plotted vs. Reynolds number in Figure 9.

7. A photograph of original Brush recorder charts for runs 210 and 211 is presented in Figure 8. The chart record for one of the gas runs is also found in Figure 8.

DISCUSSION

Effects of Equipment Parameters and Operating Techniques

Before any discussion of the effects of various parameters upon the results of this study, the reproducibility of these results for a given system and Reynolds number should be noted. For four different runs, all at a Reynolds number of 422-3, the values of E found were 6.2, 6.3, 6.3, and 6.2. Static injection was employed in all the runs.

Figure 8 is a photograph of the original Brush recorder charts for runs 210 and 211, System I-3, at a Reynolds number of 485. Run 210 was made under conditions of static injection, and dynamic injection of the dye pulse was employed in 211. The profiles are virtually identical. Reproducibility was apparently realized for the experimental conditions and methods used.

When one has established that results were reproducibile and independent of injection technique, the effect of changes in the unpacked observation gaps must be considered. To ascertain the importance of the gap, experiments in system A-3 were subdivided into (1) runs in which the light beam at station 1 passed through the column at a point 1.2 cm. below bed 1 and (2) runs in which the first station-light beam was situated 0.1 cm. below the first bed. No difference in determined coefficients resulted. Further, runs were made in system B-5 in which gap 1 was removed entirely and gap 2 served as the initial observation point. Thus X_1 was 3 ft. in these runs. Since the resulting dispersion coefficients so obtained agreed with those found with the first unpacked gap in its position between beds 1 and 2, it may be concluded that any mixing which could occur in these gaps is insignificant compared with bed mixing. When it is realized that a 2-ft. section of packed bed causes a pulse dispersion equivalent to that of about sixty perfect mixers, it is not surprising that the presence of unpacked gaps, each only 2 cm. high, contributes in no way to pulse dispersion.

In addition the 3-ft.-bed experiments would suggest that the packing method used in this work is a reproducible one for spheres, in that identical dispersion data are obtained when two independently packed beds are joined to form a 3-ft.-bed unit.

Bed Capacitance and Length

Initial two-station experiments with system A-3 revealed immediately that the amplitude ratio between stations 1 and 2, C_1/C_2, did not equal the square root of the time ratio $(t_2/t_1)^{1/2}$ as predicted by both the diffusion and cell-mixing models. The same deviation was noted in systems B-5, C-½, and D-6. Further, the magnitude of the inequality ($K_1 \neq K_2$) increased with decreasing particle size. Since theory predicts that K_1 equals K_2, the ratio K_1/K_2 as found in two-station experiments, is the indication of deviation from theory. This ratio, as a function of particle sizes studied, is listed below. These tabulated values are virtually independent of the Reynolds number.

Example	System	D_p	K_1/K_2
Run 124	D-6	6-mm. rings	1.1
67	B-5	5-mm. spheres	1.15
37	A-3	3-mm. spheres	1.23
96	C½	½-mm. spheres	2.3

The noted inequality could be explained either by an increase in E with distance or by a bed-capacitance effect which withholds a fraction of the original signal in the first bed. The evidence found to support the bed capacitance theory is:

1. The same value of E fits both station data for a given run provided one uses a value of $K_2 < K_1$ in applying Equation (17).

2. If a larger value of E is applied to station 2 data to account for the abnormal amplitude change, the resulting predicted concentration-time profile does not fit the experimental profile so well as the expression based upon constancy of E and bed capacitance. (For example, see Figure 6.)

3. Experiments with beds of ½- and 1-ft. lengths indicate that the dispersion coefficient increases with decreasing bed length. These data, when considered with the system B-5 data obtained at 2- and 3-ft.-bed lengths, which indicate constancy of E at each length, would refute the possibility of an increasing dispersion coefficient with increasing length.

4. All the data revealed the presence of long tails at each station. (For example, see Figure 7.) This would suggest a hold-back of tracer which is only slowly removed from the bed through which the pulse has just passed.

5. Gas-dispersion studies demonstrate obedience to the theoretical amplitude-length relationship, presumably because the high molecular diffusivity of the gas minimizes capacitance.

Bed Length

While these arguments tend to preclude the viewpoint of an increasing E with bed length *in the bed*, the short-bed studies might seem to point to an explanation of the amplitude discrepancy other than the bed-capacitance hypothesis. Studies of 3-mm. spheres in ½- and 1-ft. beds reveal that E decreased with bed height in the following fashion (Re = 240):

System	X, ft.	E, sq. cm./sec.
G-3	½	9
H-3	1	7
A-3	2	4.8
A-3	3	4.8

*Complete tabular material has been deposited as document 5715 with the American Documentation Institute, Photoduplication Service, Library of Congress, Washington 25, D. C., and may be obtained for $1.25 for photoprints or $1.25 for 35-mm. microfilm.

In other words the short-column data indicate an entrance effect, independent of the mode of injection as shown in Figure 8, which might be manifested when a dispersed pulse enters the second of a two-bed system. Hence an entrance effect or a reentrance effect in two-station studies may reasonably account for the discrepancy in amplitude-ratio data. With reference to Figure 4, however, it is noted that abnormally high dispersion coefficients are obtained in the ½- and 1-ft.-bed studies only at Reynolds numbers above about 20. Below this value all the data appear to align themselves with long-bed data (*A*-3) and the ½-mm. data (*C*-½). These ½-mm. data obtained in a ½-ft. bed very successfully bridge the data of systems *A*-3 and those data of Rafai (*15*) obtained in a 4-ft.-long bed as shown in Figure 3. One may conclude that in this region of flow bed length has no effect. Yet *within this region* serious discrepancies in amplitude ratio were noted in the data of the ½-mm. sphere. Thus the bed-capacitance hypothesis is not excluded by the evidence of entry effects. In addition the short-bed data suggest that E increases with decreasing bed length in the same manner for 3-, 2-, and 1-mm. particles, while the noted amplitude discrepancy is clearly a function of particle size.

It is suggested that the short-bed results are due either to the rapid acceleration of a fluid upon entering a system restricting flow, such as a packed bed, or to the inapplicability of boundary-condition equation (13) for short beds.

Consideration was given to the fact that perhaps the diffusion law cannot be applied to short beds for the reasons cited by Beeton (*3*). As discussed under Theory, the diffusion model can be applied beyond five mixing lengths. However the ½-ft. bed consists of more than five mixing lengths measured in terms of particle diameters. Even in terms of n where

$$n = Lv/2E \qquad (5)$$

the lowest value found in the ½-ft. bed studies was 8.

Influence of Controlled Variables

The effect of the Reynolds number upon the axial dispersion coefficient is immediately evident in Figures 3 and 4. When one confines his attention to the ½-, 3-mm., and Rafai's data it appears that E varies linearly with Reynolds number in the range of 0.1 to about 100. Between 100 and about 350 to 400 the exponent of the Reynolds number changes from unity to about 0.8 and then to about ¼ beyond the *break point*. This *break point* phenomenon is exhibited by all systems studied in the higher Reynolds-number range, with the exception of the 6-mm. ring system (*D*-6) where such a change in slope is not clearly evident. From a general consideration of packed-bed friction-factor characteristics and particularly with reference to the friction data determined in this study (Figure 9), it is quite clear that the *break point* in the E — Re relationship occurs in the very same Reynolds-number range as does the transition from *laminar* to *turbulent* friction-factor behavior in the f — Re relationship.

As shown in Figure 5, the cell mixing efficiency, that is, $(\gamma/2)Pe$, is independent of Reynolds number up to the transition region. The height of a mixing unit (HMU = $2E/v$) is a constant for a given system until the friction-factor–Reynolds-number transition region, at which point the intraparticle turbulence reduces the HMU value rapidly. The limit of the Peclet number, corresponding to perfect-void cell mixing, would then approach at a Reynolds number of perhaps 2,500 to 3,000. This prediction is made on the basis of Figure 5, where an extrapolation of the Pe — Re relationship to a Peclet number value of 2 brings one into the cited Reynolds-number range.

Particle Size and Shape

The effect of particles size and shape upon the dispersion coefficient is most interesting. While the data for ½-, 1-, 2-, and 3-mm. particles are apparently uniquely correlated (excluding those data for short beds) as a function of the Reynolds number, those of the 5-mm. spheres and 6-mm. rings fall below these data. When it was suspected that these 5- and 6-mm. data might be the result of a pipe-to-particle diameter ratio, a study was made of the dispersion characteristics of 3-mm. spheres in a 1-in. I.D. column. This system (*I*-3) exhibited identical dispersion characteristics with

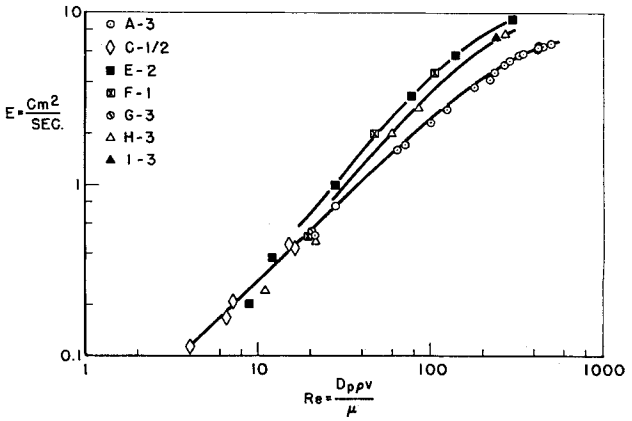

Fig. 4. E vs. Re for 1/2, 1, 2, and 3 mm. particles.

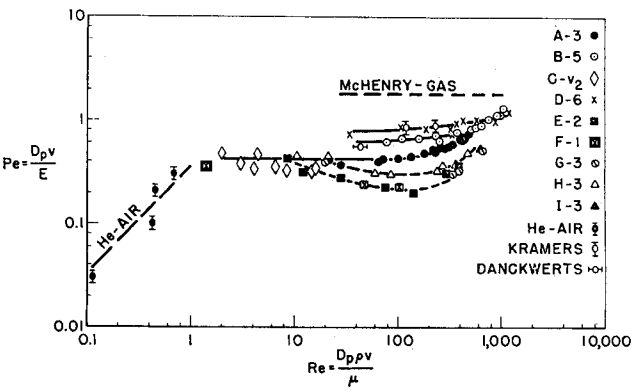

Fig. 5. Peclet number vs. Reynolds number.

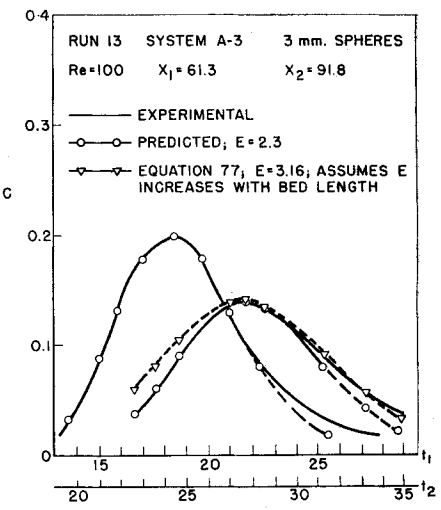

Fig. 6. Experimental and predicted profile, run 13.

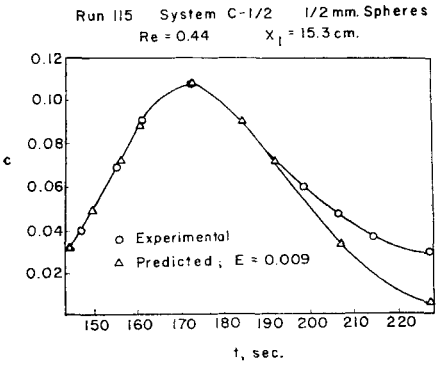

Fig. 7. Predicted and experimental profile—run 115.

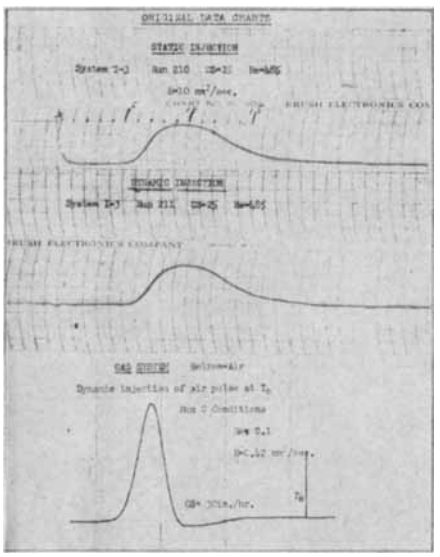

Fig. 8. Original data charts.

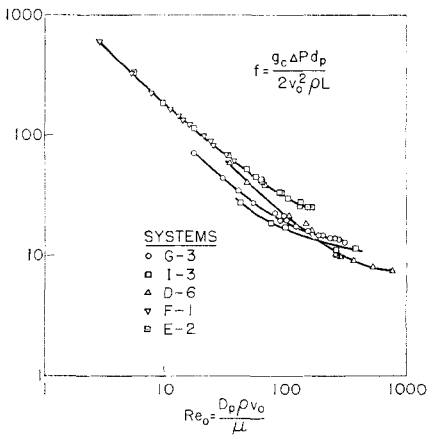

Fig. 9. Friction factor, f, vs. Reynolds number.

that of 3-mm. spheres in a 1.5-in. I.D. column (*H*-3) of equal length (1 ft.). An alternative explanation is the possibility that γ is smaller for the 5- and 6-mm. systems than for the others studied. Granting the 3-mm. sphere system an arbitrary value of $\gamma = 1$, the following values of γ result for the other systems on the basis of experimental Peclet numbers:

System	γ
½, 1, 2, 3 mm.	1
5 mm.	0.73
6 mm.	0.6

While this is an attractive hypothesis, it is difficult to see why 5-mm. spheres should pack in a manner radically different from other spheres and the 2-mm. *doughnut* rings. On the other hand the 6-mm. rings may well pack in such a fashion as to present more than one perfect mixer per particle length ($\gamma < 1$).

Referring to Figure 5, one notes that while the mixing efficiency for 6- and 5-mm. particles is greater (higher Peclet number) throughout most of the Reynolds-number range, the respective *Pe* values converge in the *turbulent* region.

It is interesting to note the similarity of the log *E* vs. log *Re* plot to a mixing-time correlation for agitated tanks and jets presented by Fox and Gex (*11*). These authors determined the time required to achieve uniformity of composition in the above-cited systems. Though their systems are radically different from those presented here, their final correlation is of note in that two regions of mixing are found, both *laminar* and *turbulent*, as noted in the present work.

In another study of miscible liquid mixing Van de Vusse (*20*) measured the mixing-time requirement in a simple tank by a pulse-injection technique and found that the mixing time varied inversely with the 0.85 power of fluid velocity. These experiments were carried out *in the absence of mechanical stirring*. Only one vessel size was investigated by Van de Vusse in this aspect of his study; thus nothing can be inferred concerning cell size. However the 0.85 exponent on flow rate applied over a thirtyfold range.

In view of these findings it is conceivable that void-cell size affects mixing efficiency in a manner more complex than is indicated by specifying cell dimension simply in terms of a particle diameter. This is to argue that the available mixing time per cell is not uniquely specified once particle diameter and bed velocity are cited, especially in the case of irregular particles such as Raschig rings. In the correlation of Fox and Gex (*11*), for example, a number of geometric factors required specification for a reasonable correlation of the data.

Pressure Drop

The pressure-drop data and friction factors calculated therefrom simply reveal the identity of transition regions for both *E* and *f* as a function of Reynolds number. No correlation between systems as far as dispersion is concerned is possible by a comparison of their respective friction-factor–Reynolds-number behavior. This point is emphasized by a comparison of the friction-factor data for 3-mm. spheres for the 1- and 1.5-in. tube systems. A change in D/D_p value results in an alteration of the $f = Re$ relationship, but no difference is noted in the dispersion characteristics of the two systems.

Previous Data

As shown in Figures 3 and 5, the results of this work are in very good agreement with the data of Rafai (*15*) and those of Kramers and Alberda (*13*). Berans's (*2*) data are very much higher than any result found in this study. Danckwerts's (*8*) value for 10-mm. Raschig rings (the same packing studied by Kramers and Alberda) falls in line with the 5-mm.–sphere results of this investigation. Values of the Peclet number reported by Klinkenberg (*12*) at Reynolds numbers "less than unity" agree well with those found in this work.

The discrepancy between phase-shift and amplitude-ratio data found by Kramers and Alberda (*13*) is interesting in that the results of the present work on amplitude-change discrepancies point to capacitance effects which would certainly cause anomalies in sinusoidal-input studies.

Gas Data

Results of the gas dispersion experiments are of an approximate nature since the dispersed pulse profiles were evaluated for the determination of *E* by using an approximate equation suitable for a Gaussian distribution. However, since the profiles were very nearly Gaussian, the *E* values so derived should not be in serious error. The Peclet numbers as determined in five experiments are plotted against the Reynolds number in Figure 5, and the gas correlation of McHenry and Wilhelm (*14*) is likewise shown there. In Figure 3 the measured *E* values for the present study are plotted vs. the Reynolds number. Within the limits of accuracy of the method of estimation the dispersion coefficients for an air pulse injected into a helium stream flowing through a packed tube appear constant. Indeed the measured values are well within the range of the molecular diffusivity of the mixture. Since an experimental value is lacking, the air-helium diffusivity was calculated by use of the Gilliland equation (*16*). On the basis of the atomic volume of helium found in a paper by Andrussow (*1*), the diffusivity of helium-air so calculated is 0.51 sq. cm./sec.

Figure 5 shows that the constancy of *E* in this system results in a linear relationship between *Pe* and *Re*. These data and those of McHenry and Wilhelm (*14*) would indicate that *Pe* must continue to increase with *Re* and gradually approach the near-limiting values found at higher Reynolds numbers by McHenry and Wilhelm.

A most interesting consequence of these limited gas studies is the indication that, at values of $Re < 1$, a value of the

molecular diffusivity of the component gas of interest in sufficient to define the dispersion characteristics of the system.

CONCLUSIONS

This study clearly demonstrates that the axial dispersion of a liquid in flow through fixed beds is of significant magnitude in the Reynolds number region below 200 to 300. With the ratio of the dispersion coefficient to average bed velocity expressed as the height of a mixing unit (HMU = $2E/v$), the data indicate constancy of this value until the flow transition regime is reached, as characterized by the packed-bed friction-factor–Reynolds-number relation. Thus the analyses of packed-bed processes (for example, ion exchange) characterized by low liquid-flow rates are rendered more complicated by this dispersion phenomenon.

The void-cell mixing model appears to substantiate the results in that low values of the Peclet number (low void-cell mixing efficiency) would be predicted in the flow region preceding fully developed void-cell turbulence, while a limiting value of Pe equal to about 2 is indicated by the model at higher Reynolds numbers. The region beyond which the height of a mixing unit decreases quite rapidly toward relative insignificance is now defined.

The Peclet number ($D_p v/E$) herein shown to be a direct measure of void-cell mixing efficiency may, with suitable modification, find useful application in stirred-tank mixing efficiency studies.

Finally the void-cell mixing model suggests that liquid kinematic viscosity effects should affect axial dispersion only insofar as the Reynolds number is modified; that is, the $E - Re$ relationship should be independent of viscosity. This point, however, requires experimental verification.

The gas data of this research and those of McHenry and Wilhelm appear to be unique in that near-perfect void-cell mixing efficiency is apparently achieved at a very low Reynolds number (about 26). However, given that the molecular diffusivity of a gas is many orders of magnitude greater than that of a liquid, it is not surprising that the ultimate in cell-mixing efficiency is achieved even at low Reynolds numbers. Indeed the data of McHenry and Wilhelm indicate an HMU $\cong$ 0.3 cm. for a bed packed with 0.3-cm. spheres. Thus in gas systems void-cell mixing is a function both of turbulence, as characterized by the Reynolds number, and of molecular diffusivity. It follows that one may expect a molecular-diffusivity contribution in liquid systems at extremely low Reynolds numbers. Indeed the data of von Rosenberg (*21*) on the displacement of benzene by *n*-butyrate from columns packed with Ottawa sand indicate dispersion coefficients about equal to liquid-molecular diffusion coefficients at flow rates of about a few feet a day.

Though data are now available over a wide range of conditions for both gases and liquids, the chief problem, namely that of mathematically defining the precise physical events which contribute to dispersion, remains unsolved. Even the simple void-cell mixing model employed here is very complex in that the ancient problem of mixing efficiency still demands rigorous mathematical description.

ACKNOWLEDGMENT

This research was supported in part by a grant from the Petroleum Research Fund administered by the American Chemical Society. Grateful acknowledgment is made to the donors of the fund. The authors are equally grateful for support provided by the Allied Chemical and Dye Corporation and the Yale Garland Fund.

William E. Kirst and Clyde O. Davis, Director and Assistant Director, respectively, of the Eastern Laboratory, Explosives Department, E. I. du Pont de Nemours and Company, most generously made this research possible by their loan of the Brush Oscillograph. George Kopperl, Edgar Slocum, and Joseph Jaffer deserve specific citation for their contributions to the design of the photocell amplifier circuit.

Richard H. Wilhelm of Princeton University very generously provided the author with the 1-mm. glass spheres employed during this study, and Martin Saunders of the Yale Chemistry Department very kindly provided the facilities for the gas dispersion study.

NOTATION

a = half-thickness of finite pulse, cm.
A = cross-sectional area of column, sq. cm.
C = tracer concentration, ml. standard/ml. of solution
D_p = particle diameter, cm.
D = nominal column diameter, cm.
D_m = molecular diffusivity, sq. cm./sec.
ϵ = cell mixing efficiency = $(2/\gamma)Pe$.
E = axial dispersion coefficient, sq. cm./sec.
f = packed bed friction factor
f = void fraction
HMU = height of a mixing unit, cm.
I.D. = inside diameter of column, cm.
k = proportionality constant
K = coefficient of Equation (17)
K' = coefficient, $K' = K\sqrt{E}$
L = bed length, cm.
n = number of mixers, $Lv/2E$
n_p = number of perfect mixers $L/\gamma D_p$
Pe = Peclet number, $D_p v/E$
Q = quantity of tracer injected
r = column radius, cm.
Re = Reynolds number, $D_p v\rho/\mu$
t = time, sec.
T = total retention time
t_m = actual time of pulse maximum, $X/v - E/v^2$, sec.
v = average bed velocity, cm./sec.
v_0 = superficial velocity, cm./sec.
X = packed bed distance, cm.
Z = change of variable = $X - vt$, cm.

Greek Letters

γ = fraction of a particle diameter equal to a perfect mixing length
ρ = density, g./cc.
θ = holding time, sec.
θ_n = cell holding time, sec.
σ = standard deviation, cm.
μ = viscosity, g./(cm.)(sec.)
erf = error function

Subscripts

1, 2 = observation point references

LITERATURE CITED

1. Andrussow, Leonid, *Z. fur physik. chem.*, **199**, 314 (1952).
2. Aris, Rutherford and Neal R. Amundson, *A.I.Ch.E. Journal*, **3**, No. 2,280 (1957).
3. Beeton, A. B. P., *Brit. Natl. Gas Turbine Establishment, Report* R 152 (March, 1954).
4. Beran, M. J., Ph.D. dissertation, Harvard Univ., Cambridge, Mass. (May, 1955).
5. Bernard, Robert A., and Richard H. Wilhelm, *Chem. Eng. Progr.*, **46**, No. 5, 233 (1950).
6. Bretton, R. H., personal communication (September, 1956).
7. Carberry, J. J., *A.I.Ch.E. Journal*, **4**, 13M (1958).
8. Danckwerts, P. V., *Chem. Eng. Sci.*, 2, 1 (1953).
9. Ergun, Sabri, *Chem. Eng. Progr.*, **48**, No. 5, 227 (1952).
10. Ferrell, J. K., *et al.*, *Ind. Eng. Chem.*, **47**, No. 1, 29 (1955).
11. Fox, E. A., and V. E. Gex, *A.I.Ch.E. Journal*, **2**, No. 4, 539 (1956).
12. Klinkenberg, A., and F. Sjenitzer, *Chem. Eng. Sci.*, **5**, No. 6, 258 (1956).
13. Kramers, H., and G. Alberda, *Chem. Eng. Sci.*, 2, 173 (1953).
14. McHenry, K. W., and R. H. Wilhelm, *A.I.Ch.E. Journal*, **3**, No. 1, 83 (1957).
15. Rafai, Mohamed N. E., Ph.D. dissertation, Univ. Calif., Berkeley (1956).
16. Sherwood, T. K., and R. L. Pigford, "Absorption and Extraction, p. 10, McGraw-Hill Book Company, Inc., New York (1952).
17. Smith, J. M., *et al.*, *Ind. Eng. Chem.*, **45**, 1209 (1953).
18. Taylor, G. I., *Proc. Roy. Soc.*, **A225**, 473 (1954).
19. Van Deemter, J. J., *et al.*, *Chem. Eng. Sci.*, **5**, No. 6, 271 (1956).
20. Van de Vusse, J. G., *ibid.*, **4**, 209 (1955).
21. Von Rosenberg, D. U., *A.I.Ch.E. Journal*, **2**, No. 1, 55 (1956).

Manuscript received Sept. 4, 1957; revision received Jan. 28, 1958; paper accepted Jan. 30, 1958.